

Structure of a Human Inositol 1,4,5-Trisphosphate 3-Kinase: Substrate Binding Reveals Why It Is Not a Phosphoinositide 3-Kinase

Beatriz González,¹ Michael J. Schell,³
Andrew J. Letcher,³ Dmitry B. Veprintsev,²
Robin F. Irvine,³ and Roger L. Williams^{1,*}

¹MRC Laboratory of Molecular Biology and

²Centre for Protein Engineering

Hills Road

Cambridge CB2 2QH

United Kingdom

³Department of Pharmacology

University of Cambridge

Tennis Court Road

Cambridge CB2 1PD

United Kingdom

Summary

Mammalian cells produce a variety of inositol phosphates (InsPs), including Ins(1,4,5) P_3 that serves both as a second messenger and as a substrate for inositol polyphosphate kinases (IPKs), which further phosphorylate it. We report the structure of an IPK, the human Ins(1,4,5) P_3 3-kinase-A, both free and in complexes with substrates and products. This enzyme catalyzes transfer of a phosphate from ATP to the 3-OH of Ins(1,4,5) P_3 , and its X-ray crystal structure provides a template for understanding a broad family of InsP kinases. The catalytic domain consists of three lobes. The N and C lobes bind ATP and resemble protein and lipid kinases, despite insignificant sequence similarity. The third lobe binds inositol phosphate and is a unique four-helix insertion in the C lobe. This lobe embraces all of the phosphates of Ins(1,4,5) P_3 in a positively charged pocket, explaining the enzyme's substrate specificity and its inability to phosphorylate PtdIns(4,5) P_2 , the membrane-resident analog of Ins(1,4,5) P_3 .

Introduction

Inositol phosphates (InsPs) are a highly diverse group of molecules, at least thirty of which occur in mammalian cells (for review see Irvine and Schell, 2001). With the exception of the second messenger Ins(1,4,5) P_3 (Berridge, 1993), the physiological functions of many InsPs are as yet incompletely understood. Following its liberation from the lipid phosphatidylinositol 4,5-bisphosphate, Ins(1,4,5) P_3 can be further metabolized to more highly phosphorylated InsPs, whose proposed functions in cells are diverse and include roles in chemotaxis, vesicular trafficking, channel regulation, cell proliferation, and a variety of nuclear functions (Irvine and Schell, 2001). InsP synthesis occurs by sequential phosphorylations catalyzed by different InsP kinases, many of which have been cloned.

Based on sequence similarities, InsP kinases fall into three major families. The largest family is the inositol polyphosphate kinases (IPKs; PFAM accession PF03770),

which includes Ins P_6 kinases (IP $_6$ -Ks) (Saiardi et al., 1999; Schell et al., 1999), InsP "multi-kinases" (IPmKs) (Chang et al., 2002; Odom et al., 2000; Saiardi et al., 1999; Shears, 2004), and Ins(1,4,5) P_3 3-kinases (IP $_3$ -3Ks) (Choi et al., 1990; Communi et al., 1995; Dewaste et al., 2000; Irvine et al., 1986; Pattni and Banting, 2004). A second family, the Ins(1,3,4) 5/6-kinases (also known as Ins(3,4,5,6) P_4 1-kinases), is also widespread, especially in plant genomes (Ho et al., 2002; Shears, 2004; Wilson and Majerus, 1996). The third family, the Ins(1,3,4,5,6) P_5 2-kinases, appears to have fewer members, at least based on sequence homologies (Ives et al., 2000; Verbsky et al., 2002; York et al., 1999). Sequence analyses suggest that Ins(1,3,4) P_3 5/6-kinases belong to the ATP-grasp fold family (Cheek et al., 2002), but no three-dimensional structure has been reported for any InsP kinase.

The IP $_3$ -3Ks are the most recent evolutionary branch of the IPK family, since they are confined to metazoans (Irvine and Schell, 2001; Pattni and Banting, 2004) and appear to have evolved about the same time as Ins(1,4,5) P_3 receptors. IP $_3$ -3Ks have an exquisite specificity for Ins(1,4,5) P_3 as a substrate and phosphorylation of the 3-OH as the reaction (Bird et al., 1992; Irvine et al., 1986; Morris et al., 1988). They have three potential functions. (1) They catalyze the removal of Ins(1,4,5) P_3 , thereby terminating the signal to release calcium from intracellular stores. Genetic evidence in support of the physiological importance of this function has come from targeted disruptions of the IP $_3$ -3K in *C. elegans* and the A isoform in mice (Clandinin et al., 1998; Jun et al., 1998). (2) Another function is to produce Ins(1,3,4,5) P_4 , which has a probable but presently unclear physiological function (Irvine and Schell, 2001). Support for the physiological importance of Ins(1,3,4,5) P_4 has come from mice lacking the B isoform of IP $_3$ -3K, which are defective in T-lymphocyte development (Pouillon et al., 2003; Wen et al., 2004). This function might be mediated by GAP1^{IP4BP}, a putative Ins(1,3,4,5) P_4 receptor (Cullen et al., 1995), highly expressed in T cells (Wen et al., 2004). (3) The third possible function of IP $_3$ -3Ks is to serve as a starting point for the synthesis of all the other higher-phosphorylated inositol phosphates in mammals, though there is evidence both for and against this (Balla et al., 1994; Irvine and Schell, 2001; Shears, 2004).

There are three IP $_3$ -3Ks encoded by the human genome, A, B and C (Communi et al., 1995; Dewaste et al., 2003; Irvine and Schell, 2001; Pattni and Banting, 2004); they all have a similar C-terminal catalytic domain that also shares common structural features with other IPKs, the IP $_6$ -Ks and IPmKs. In addition, animal IP $_3$ -3Ks also have a conserved Ca²⁺/Calmodulin (CAM) binding domain (Communi et al., 1995). By contrast, the N-terminal regions of IP $_3$ -3Ks are highly divergent and govern cellular targeting (Dewaste et al., 2003; Pattni and Banting, 2004). Isoform A predominates in neurons and in testis (Mailleux et al., 1991; Yamada et al., 1992) and is localized to dendritic spines by an association with filamentous actin (Schell et al., 2001), consistent with its probable contribution to memory functions (Jun et al., 1998). Isoform B is expressed widely, and it is in the

*Correspondence: rlw@mrc-lmb.cam.ac.uk

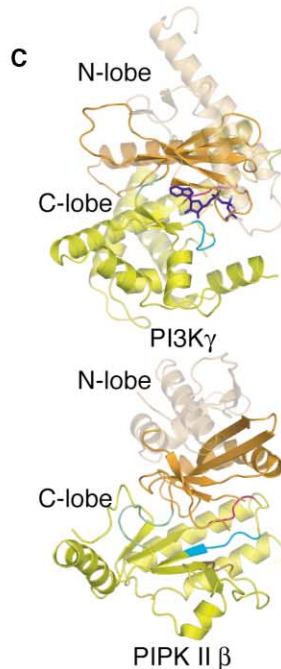
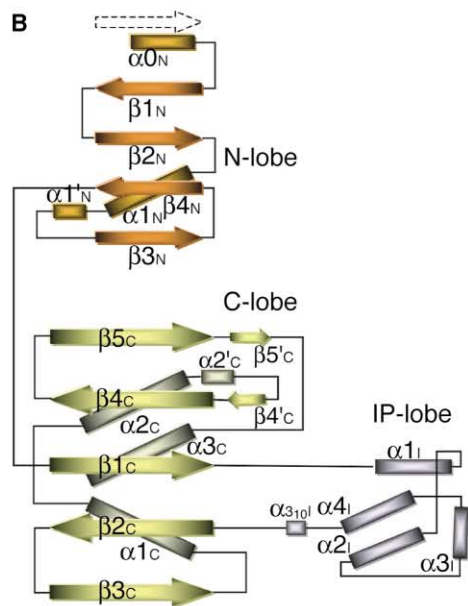
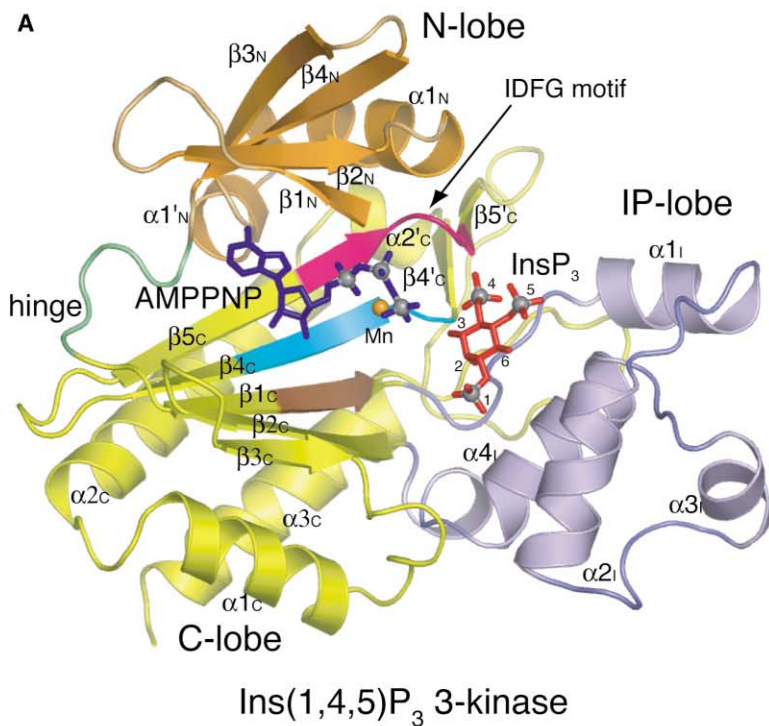


Figure 1. The Overall Fold of IP₃-3K Catalytic Domain

(A) A ribbon diagram of IP₃-3K in a complex with Mn²⁺/AMPPNP/Ins(1,4,5)P₃. The N lobe is colored orange, the C lobe yellow, the IP lobe purple, and the hinge green. The conserved IDFG, GSSLL, and DxK motifs are colored pink, cyan, and brown, respectively. This and all other molecular illustrations were prepared with PYMOL.

(B) A topology diagram of the catalytic domain. Helix $\alpha 0_N$ is ordered only in the absence of substrates or products. The dashed arrow indicates an additional strand that would be characteristic of the N lobes of PKs.

(C) Ribbon diagrams of the catalytic domains of PI3K γ and PIPKII β with N and C lobes colored as in (A).

cytosol and as well as associated with the endoplasmic reticulum and with actin (Pattni and Banting, 2004). Isoform C is also expressed in many tissues and is partly nuclear (Dewaste et al., 2003; Nalaskowski et al., 2003); it is activated by CAM to a lesser degree than the A or B isoforms (Dewaste et al., 2000).

Three-dimensional structures have been determined for two types of inositol lipid kinases, the type IB phosphoinositide 3-kinase (PI3K γ ; Walker et al., 1999) and the type II β PtdInsP kinase (PIP KII β) (Rao et al., 1998).

However, neither of these have any close sequence similarity with any InsP kinases. Here we describe the structure of the catalytic part of the A isoform of IP₃-3K. Our structures of the ternary complexes of this enzyme with substrates (Mn²⁺/ATP analog/Ins(1,4,5)P₃) and with products (Mn²⁺/ADP/Ins(1,3,4,5)P₄) serve as a paradigm for all IP₃-3K isoforms and provide a framework for understanding the substrate specificity and catalysis of the entire IPK family. The structure also suggests a model for Ca²⁺/CAM activation.

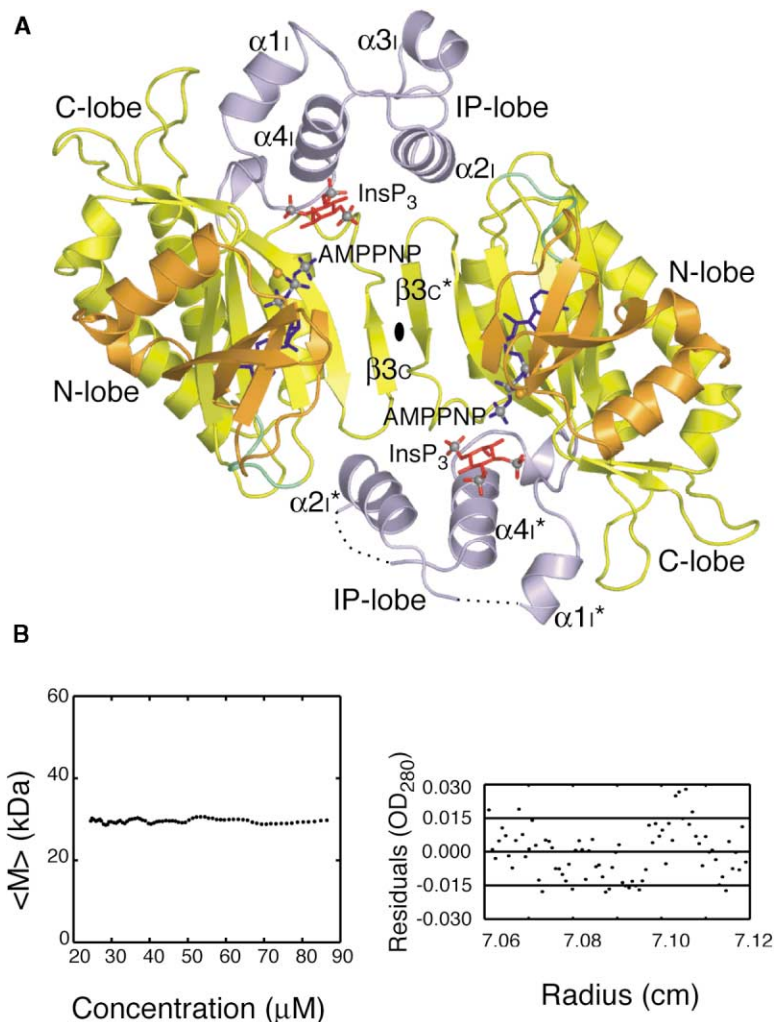


Figure 2. The Asymmetric Unit of the IP₃-3K Crystal Contains a Dimer, but the Construct Is a Monomer in Solution

(A) A ribbon diagram of the IP₃-3K dimer with the dyad axis indicated.

(B) The average mass $\langle M \rangle$ of the IP₃-3K as a function of protein concentration as determined by analytical centrifugation (left) and a plot of the residuals (A_{280} observed - A_{280} calculated) as a function of radius along the cell.

Results and Discussion

IP₃-3K Structure

We have determined the structure of the catalytic domain of human IP₃-3K A (residues 187 to 461) in the apo-form and the holo-form (with either substrates or products in the active site). The kinase domain can be divided into three subdomains, an $\alpha + \beta$ N-terminal subdomain that we will refer to as the N lobe, an $\alpha + \beta$ C-terminal subdomain that we will refer to as the C lobe and a third α -only subdomain (Figures 1A and 1B and Supplemental Figure S1). The N and C lobes and the hinge connecting them are involved primarily in binding the nucleotide and metal co-factor, while the α -helical subdomain is involved in Ins(1,4,5) P_3 binding and will be referred to as the inositol phosphate (IP) binding lobe. There are two molecules in the asymmetric unit of the crystal that are related by a dyad axis (Figure 2).

The N lobe comprises residues 187-253 and is formed by four anti-parallel β strands ($\beta 1_N$ to $\beta 4_N$) and one α -helix ($\alpha 1_N$). The β sheet has a strand order 1-2-4-3, with $\alpha 1_N$ forming a crossover connection between $\beta 2_N$ and $\beta 3_N$ (Figure 1B). The N-terminal residues form a small $\alpha 0_N$ helix in the apo-form (residues 187-196) that is disor-

dered when substrates or products are bound. In the apo-form, this N-terminal helix occupies much of the volume of the ATP binding pocket (Figure 3D).

The C lobe is formed by residues 254-265 and 330-461. It has an $\alpha + \beta$ fold where a five-stranded anti-parallel β sheet with a 5-4-1-2-3 strand order forms the core of the lobe (Figure 1B). The $\beta 4_C$ and $\beta 5_C$ strands connect via a kink to the small two-stranded antiparallel β sheet, consisting of $\beta 4'_C$ and $\beta 5'_C$, that extends beyond the β sheet core. The five-stranded β sheet is stabilized by the three α helices bracing the back of the lobe ($\alpha 1_C$ and $\alpha 2_C$, which connect the $\beta 3_C$ and $\beta 4_C$ strands, and the C-terminal $\alpha 3_C$).

The IP binding lobe has a well-defined, independent structure formed by a long insertion in the C lobe (residues 266-329). This lobe, consisting of four α helices ($\alpha 1_i$ - $\alpha 4_i$) forming a left-handed coil, emerges from the C lobe and connects strands $\beta 1_C$ and $\beta 2_C$. The IP binding lobe interacts through its N-terminal portion with a substructure formed in the C lobe by $\beta 4'_C$ and the elaborate loop between $\beta 5'_C$ and $\alpha 3_C$. This substructure provides a support to the IP binding lobe through several interactions, including a salt bridge between Arg279 and Glu437. The IP lobe and the N-terminal residues of the construct

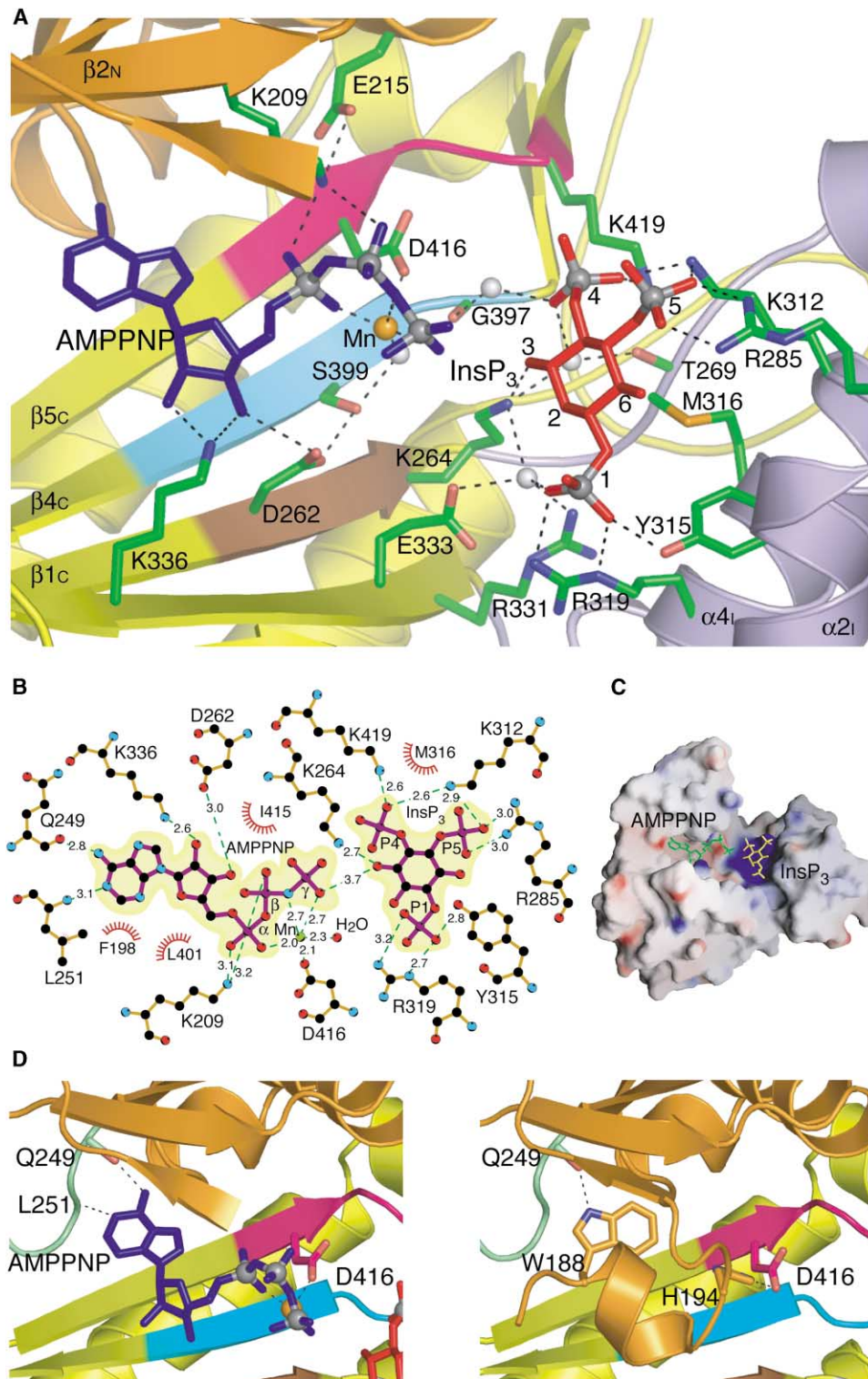


Figure 3. Substrate Binding by IP₃-3K
 (A) A view of the active site showing the ATP analog and Ins(1,4,5)P₃ bound to the enzyme. The subdomains and motifs are colored as in Figure 1. Side chains interacting with the ligands are shown as sticks and ligand-bound water molecules as white spheres.
 (B) A schematic of the interactions with the ligands made with LIGPLOT.
 (C) A surface illustration of the IP₃-3K catalytic domain colored by electrostatic potential with negatively charged regions red and positive blue. The bound AMPPNP is shown as green sticks and the Ins(1,4,5)P₃ as yellow sticks.
 (D) A close-up of the ATP binding pocket in the presence of AMPPNP (left) and in its absence (right), showing Trp188 and His194 from the putative auto-inhibitory region mimicking the interactions formed by ATP.

are the most flexible portions of the enzyme, judging from the temperature factors. The IP binding lobe is partially disordered in one of the two molecules in the asymmetric unit (Figure 2A).

The dimer in the asymmetric unit is formed by 2-fold symmetric contacts that include strand $\beta 3_c$, the $\beta 2_c$ - $\beta 3_c$ loop and helix $\alpha 2$, (Figure 2A). The dimer interface buries 1433 Å² of surface area and involves 22 hydrogen bonds. Nevertheless, analytical ultracentrifugation shows that the construct crystallized is a monomer in solution (Figure 2B).

Substrate Binding

Soaking experiments with native crystals have allowed us to determine the structures of ternary complexes with substrates ($Mn^{2+}/AMPPNP/Ins(1,4,5)P_3$) and products ($Mn^{2+}/ADP/Ins(1,3,4,5)P_4$). Product complexes were obtained by either soaking crystals with products or by soaking crystals with substrates and forming the products in situ. Therefore, the construct crystallized has kinase activity under the crystallization conditions.

ATP Binding

The ATP binding cleft is situated between the N and C lobes, with the adenine moiety hydrogen bonded to the main chain of residues Gln249 and Leu251 (Figures 1A and 3). The hydrophobic pocket for the adenine and ribose is formed by residues from the hinge (Leu251 and Leu252) together with residues from the N lobe (Phe198) and from the C lobe (Leu401 and Ile415, parts of the highly conserved GSSLL₄₀₁ and I₄₁₅DFG motifs, respectively). The ribose oxygens of the ATP are hydrogen bonded to the side chains of Lys336 and Asp262. Asp262 is in the signature D₂₆₂XK motif fully conserved among members of the IPK family (Figures 1A and 3A). However, a D262A mutant retains significant activity (Table 2), suggesting that this residue does not have a major role in catalysis. The equivalent of Lys336 was mutated to Gln in the chicken IP₃-3K leading to an increase in Km for ATP (Bertsch et al., 2000). The residues coordinating the ATP phosphates are absolutely conserved among the members of the IP₃-3K family. Lys209 from $\beta 2_N$ is coordinated to the α - and β -phosphates (Figure 3A). The strictly conserved Asp416 among IPKs (from the ID₄₁₆FG motif) coordinates the α and γ phosphates via the Mn^{2+} co-factor. This aspartate seems to position the γ phosphate for subsequent nucleophilic attack by the 3-OH. The importance of these interactions is seen in the complete loss of activity in the D416A mutant (Table 2). Mutation of the analogous residue in the rat IP₃-3K (D414Q) also led to inactive enzyme (Communi et al., 1995). The coordination sphere of the metal also includes one ordered water molecule that is in turn hydrogen-bonded to Ser 399, part of the conserved GSS₃₉₉LL motif that is required for enzymatic activity (Dubois et al., 2002; Saiardi et al., 2001).

An earlier report had suggested that Lys199 was involved in ATP binding based on results obtained with a K199I mutation (Communi et al., 1993). The structure shows that Lys199 is not near the ATP binding site and the essentially wild-type activity of the K199A mutant (Table 2) suggests that the effect of the K199I mutation may have been due to this more drastic mutation being

deleterious to proper folding of the enzyme. Moreover, this residue is not conserved in all IP₃-3Ks.

InsP Binding

Previous structural studies of phosphoinositide kinases did not provide direct information about inositide binding due to difficulties of crystallizing the kinases with lipid or soluble substrate analogs (Rao et al., 1998; Walker et al., 1999). The crystal structures of the substrate and product complexes of IP₃-3K offer the first view of inositide binding to a kinase. The other Ins(1,4,5) P_3 binding proteins with known structures, PH domains (Lemmon and Ferguson, 2001) and the Ins(1,4,5) P_3 -receptor (Bosanac et al., 2002), do not share any structural homology in the binding site.

The Ins(1,4,5) P_3 is well ordered, and the extensive network of interactions with the enzyme (Figures 3A and 3B) is consistent with the high affinity (Km 0.2-2 μ M) and specificity that the enzyme shows for this substrate. Most of the residues interacting directly with Ins(1,4,5) P_3 come from the IP binding lobe, especially helix $\alpha 4$. Only two residues outside the IP lobe (Lys264 and Lys419 from the C lobe) interact with the bound Ins(1,4,5) P_3 .

At physiological pH, it has been determined that the doubly ionized form of all three Ins(1,4,5) P_3 phosphates is important for interaction with IP₃-3K, and this is consistent with the interactions that we see in the structure (Yoshimura et al., 1999). The structure shows that a cluster of basic residues provides a positively charged pocket into which the Ins(1,4,5) P_3 fits (Figure 3C). Met316 forms a hydrophobic floor for this pocket against which the face of the inositol ring packs.

The 1-phosphate interacts with Arg319, Tyr315, and a water that makes three interactions with the enzyme. The importance of the 1-phosphate interactions is consistent with the observation that the R319D and R319A mutations inactivate the enzyme (Table 2). The presence of these interactions with the 1-phosphate and the orientation of the 1-phosphate in the IP binding lobe explains the observation that glycerophosphoryl-myo-inositol 4,5-bisphosphate (GroPIns(4,5) P_2) is an extremely poor substrate (Bird et al., 1992). Modeling PtdIns(4,5) P_2 in the binding pocket suggests that the lipid moiety would make severe steric clashes with helix $\alpha 2$. Crucially, these interactions would preclude IP₃-3K from interacting with phosphoinositides. The inability of IP₃-3K to generate PtdIns(3,4,5) P_3 contrasts with the PtdIns(4,5) P_2 3-kinase activity of some IPmKs (see below).

The 4-phosphate interacts with Lys312 and Lys419, while the 5-phosphate is coordinated by Arg285 and Lys312. These interactions impart the Ins(1,4,5) P_3 specificity of the enzyme. Mutation of the equivalent of Lys312 in the chicken Ins(1,4,5) P_3 -3K greatly decreases the apparent affinity of the enzyme for Ins(1,4,5) P_3 (Bertsch et al., 2000).

The 3-OH, which serves as the phosphate acceptor, interacts with Lys264 from the D₂₆₂XK motif. In the product complex, Ins(1,3,4,5) P_4 makes the same interactions as Ins(1,4,5) P_3 , except for an additional hydrogen bond between Lys264 and a non-bridging oxygen of the 3-phosphate (Supplemental Figure S2). Lys264 probably neutralizes the negative charge developed as the phosphate transfers to the 3-OH. Mutagenesis of Lys264

Table 1. Data Collection, Structure Determination, and Refinement Statistics

Data Collection and MAD Phasing Statistics					
Data set	TMLA MAD Phasing		Native Enzyme DataPeak ^c		
	Peak ^c	Inflection ^c	Apoenzyme	Substrate Complex	Product Complex
Resolution	1.80 Å	1.80 Å	1.80 Å	1.95 Å	1.94 Å
Completeness (last shell)	100.0 (99.9)	99.8 (99.9)	94.7 (84.22)	98.7 (99.9)	97.2 (98.2)
R _{merge} ^a (last shell)	0.10 (0.44)	0.077 (0.29)	0.083 (0.31)	0.065 (0.30)	0.052 (0.21)
Redundancy (last shell)	13.6 (13.0)	7.0 (6.6)	6.1 (5.9)	6.7 (4.9)	6.8 (6.3)
<I/σ> (last shell)	21.3 (4.8)	14.6 (3.1)	4.9 (2.3)	7.1 (2.3)	8.5 (3.6)
Phasing statistics					
Phasing power (iso) ^b	NA	0.3			
Phasing power (anom) ^b	1.4	0.7			
Pb sites found	13				
FOM after SHARP	0.32				
FOM after SOLOMON	0.79				
FOM after DM	0.94				
Refinement Statistics					
Data set	Apoenzyme		Substrate Complex		Product Complex
Resolution (Number of reflections)	45.17-1.80 Å (48647, no cutoff)		48.80-1.95 Å (43968, no cutoff)		48.80-1.94 Å (46068, no cutoff)
Protein atoms	4404		4164		4138
Waters	265		324		259
R _{cryst} ^d	20.2		19.9		22.6
R _{free} ^d (% data used)	24.1 (5)		24.3 (5)		26.7 (5)
r.m.s.d. from ideality ^e					
bonds/angles/dihedrals	0.021/1.655/6.589		0.016/1.586/6.554		0.019/1.751/6.946
Average B (Wilson B factor)	23 (28)		21 (29)		29 (28)
RMSD B for bonded main (side) chain atoms	0.93 (2.88)		0.92 (2.37)		1.09 (2.64)

^a $R_{\text{merge}} = \frac{\sum_{hkl} \sum_i |I_i(hkl) - \langle I(hkl) \rangle|}{\sum_{hkl} \sum_i I_i(hkl)}$.

^b The phasing power is defined as the ratio of the r.m.s. value of the heavy atom structure factor amplitudes to the r.m.s. value of the lack-of-closure error.

^c Data sets were collected at ESRF beamline ID14-4 at wavelengths 0.9492 Å and 0.9511 Å for the peak and inflection data sets, respectively.

^d R_{cryst} and $R_{\text{free}} = \frac{\sum |F_{\text{obs}} - F_{\text{calc}}|}{\sum F_{\text{obs}}}$; R_{free} calculated with the percentage of the data shown in parentheses.

^e r.m.s. deviations for bond angles and lengths in regard to Engh and Huber parameters.

shows a complete loss of activity (Togashi et al., 1997), consistent with this residue having a major role in catalysis as suggested by the structure. Although the 2- and 6-hydroxyls make no direct hydrogen bonds to the enzyme, the presence of Met316 and Met288 near the 2- and 6-hydroxyls would prevent binding of inositol phosphates phosphorylated at these positions.

Similarity to Protein and Lipid Kinases

A search with the DALI server identified lipid and protein kinases as having folds most similar to IP₃-3K. The basic elements of the protein kinases (PK) N lobes (Cheek et al., 2002) are a five stranded anti-parallel β sheet and an α-helix [αC in the cAMP-dependent protein kinase (PKA) nomenclature that will be used as a reference for PKs] (Taylor and Radzio-Andzelm, 1994). IP₃-3K has these structural elements except that the N lobe has helix α0_N instead of an N-terminal β strand (Figure 1B) and that this region is disordered in the presence of bound ATP or ADP. This difference between IP₃-3K and PKs in the N lobe could be the consequence of this N-terminal segment being involved in Ca²⁺/CAM activation of the enzyme (see below). Although the lack of a β strand analogous to the first strand of the PK N lobe might be an artifact of the N-terminal deletion that we used, this construct has a catalytic activity as great as the intact enzyme (Takazawa and Erneux, 1991).

Several key features of the IP₃-3K N lobe suggest homology with PKs. There is a salt bridge between Lys209 at the end of β1_N (equivalent to Lys72 in PKA) and Glu215 in α1_N (Glu91 in αC of PKA). The presence of this bridge is one of the hallmarks of an active conformation of the PKs (Huse and Kuriyan, 2002). In addition, the above lysine coordinates the ATP phosphates in both enzymes. In IP₃-3K, there is a loop (Q₁₉₀LAGHTG) equivalent to the glycine-rich loop (G loop) of the PKs. This loop is disordered in the ATP bound crystal structure of IP₃-3K, and high mobility for the G loop in PKs also has been previously reported (Madhusudan et al., 1994). In the IP₃-3K apo form, this loop connects α0_N with β1_N, instead two β strands as in PKs, and has features that are unique for IP₃-3K as discussed below. Analogous to the PKs, the N and C lobes are connected by a hinge that forms part of the walls of the ATP binding cavity and key interactions with the adenine base (Taylor and Radzio-Andzelm, 1994).

The IP₃-3K C lobe is notably different from PKs, although a few key elements are conserved. The C lobe is an α+β domain in both PKs and IP₃-3K, but the principal feature of this lobe in IP₃-3K is a large β sheet. In contrast, the C lobes of PKs and phosphoinositide 3-kinase are primarily α-helical (Figure 1C). At the heart of the IP₃-3K C lobe is a (α2/β4'β4/β5β5')_C core analogous to a conserved segment essential for ATP binding in the

Table 2. Activities of IP₃-3K Mutants

Mutant	Activity (% wild-type)
W188A	44%
K199A	80%
D262A	14%
D262N	12%
R319D	ND
R319A	0.5%
D416A	ND

ND = no activity detected. Mutants were assayed as described previously (Dewaste et al., 2000) at low (approx 4 nM) Ins(1,4,5) P_3 , 1 mM ATP, and at the same protein concentration as wild-type, or additionally at 100 \times higher protein concentration for the last three mutants. Assays were carried out using a construct containing the calmodulin-binding domain and the catalytic domain (residues 157-461). The data shown are representative of three independent experiments and are the averages of duplicate measurements. More quantitative kinetic characterization was prevented by Ins(1,4,5) P_3 substrate inhibition, which was exhibited by the construct (data not shown). This phenomenon has been reported for a truncated C isoform (Nalaskowski et al., 2003), but not the full-length enzyme (Dewaste et al., 2000). The construct used in generating the above IP₃-3K isoform A mutants was truncated in a place similar to one used for the C isoform (Nalaskowski et al., 2003). The observed substrate inhibition by Ins(1,4,5) P_3 and non-linear kinetics with ATP (data not shown) may be caused by a requirement for ATP to bind before Ins(1,4,5) P_3 . From experiments at low Ins(1,4,5) P_3 concentrations, the K_m and V_{max} of the wild-type enzyme can be estimated to be approximately 1.1 μ M and 30 μ moles/min/mg protein, respectively.

C lobes of PKs (Grishin, 1999) (Figure 4). Part of this core is an ID₄₁₆FG motif between $\beta 5_c$ and $\beta 5'_c$ (Figure 4A), which is topologically equivalent to the D₁₈₄FG motif between $\beta 8$ and $\beta 9$ in PKA. This motif and the subsequent loop has been referred to as the activation loop in PKs (Figure 4B). In both IP₃-3K and PKs, the aspartates in this motif have the same role, positioning the γ -phosphate of ATP through a metal-mediated interaction. Another key element of PKs, known as the catalytic loop, is absent in IP₃-3K (Figure 4B). The catalytic loop in PKA is characterized by a D₁₆₆xKxxN motif, which forms a prominent protrusion between strands $\beta 6$ and $\beta 7$ (Figure 4B). Asp166 of PKA has been proposed to orient the OH of the serine substrate, while Lys168 neutralizes the charge developed in catalysis by coordinating the γ -phosphate of ATP before and after transfer (Madhusudan et al., 2002). The topological equivalent to the catalytic loop of PKs in IP₃-3K is in the $\beta 4'_c$ - $\beta 4_c$ region. This region differs from PKs in two respects: (1) IP₃-3K has a small kink, rather than a distinct loop and (2) IP₃-3K has a GSSLL₄₀₁ motif, which is one of the signature motifs that has been noted in all IPKs, rather than the D₁₆₆xKxxNLL motif of the PKs (Figure 4A). Outside the conserved ($\alpha 2/\beta 4'_c/\beta 4_c/\beta 5\beta 5'$) core, IP₃-3K contains another signature motif, the DxK₂₆₄ motif located in the neighboring strand $\beta 1_c$ (Figure 4A). When superimposing PKA on IP₃-3K, the Lys168 from the long catalytic loop in PKA reaches into the space occupied by Lys264 from the $\beta 1_c$ of IP₃-3K (Figures 4A and 4B). Consequently, it appears that these lysine residues have a similar function. In contrast, the aspartate residues of the DxK motifs are neither spatially nor functionally equivalent (Figures 4A and 4B).

Concerning the lipid kinases, no further structural sim-

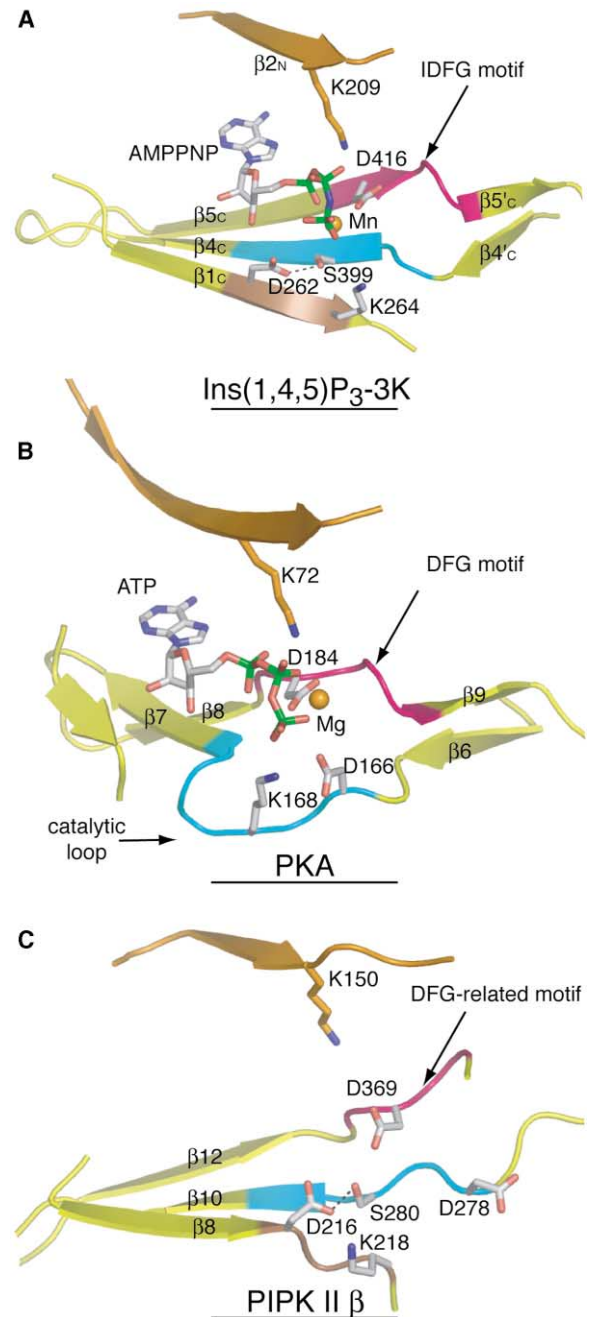


Figure 4. A Comparison of Selected Elements in the Catalytic Core of the Protein and Inositol Kinases

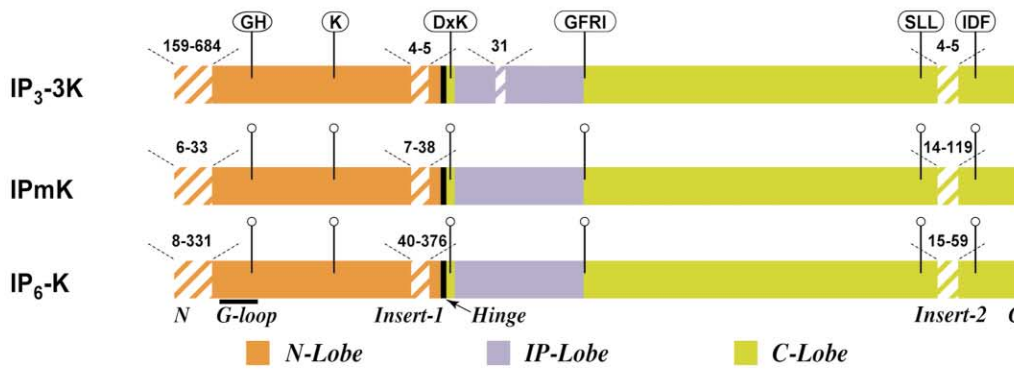
The lack of a catalytic loop and the presence of an extended β sheet in the C lobe place the IP₃-3K and PIPKII β in a subfamily of PKs that have C lobes similar to the ATP-grasp C lobe. (A) IP₃-3K with the conserved N lobe residue Lys209, which interacts with the phosphates of the ATP colored orange, the C lobe IDFG motif that interacts with the metal cofactor colored pink, the GSSLL motif corresponding to the PKA catalytic loop cyan and the DxK motif which stabilizes the transferred phosphate colored brown. (B) The analogous elements for PKA and (C) for PIPKII β .

ilarity of IP₃-3K with PI3K is evident beyond what is revealed with PKs (Figure 1C). However, phosphatidylinositol phosphate kinase II β (PIPKII β) (Rao et al., 1998)

A

Substrate	I(4,5)P ₂	I(1,4,5)P ₃		I(1,4,5,6)P ₄	I(1,3,4,5)P ₄	I(1,3,4,6)P ₄	I(1,2,3,4,6)P ₅	I(1,3,4,5,6)P ₅	IP ₆	Motifs		
Catalytic activity	1-K	3-K	6-K	3-K	6-K	5-K	5-K	5P-K	5P-K	DxK	IP-lobe	IDFG
IP ₃ -3K		✓										
IPmK	✓											
ARG82		✓	✓		✓	✓			✓			
IPmK			✓		✓	✓						
IP ₆ -K1									✓			
IP ₆ -K2										✓		
KCS1										✓		

B



C

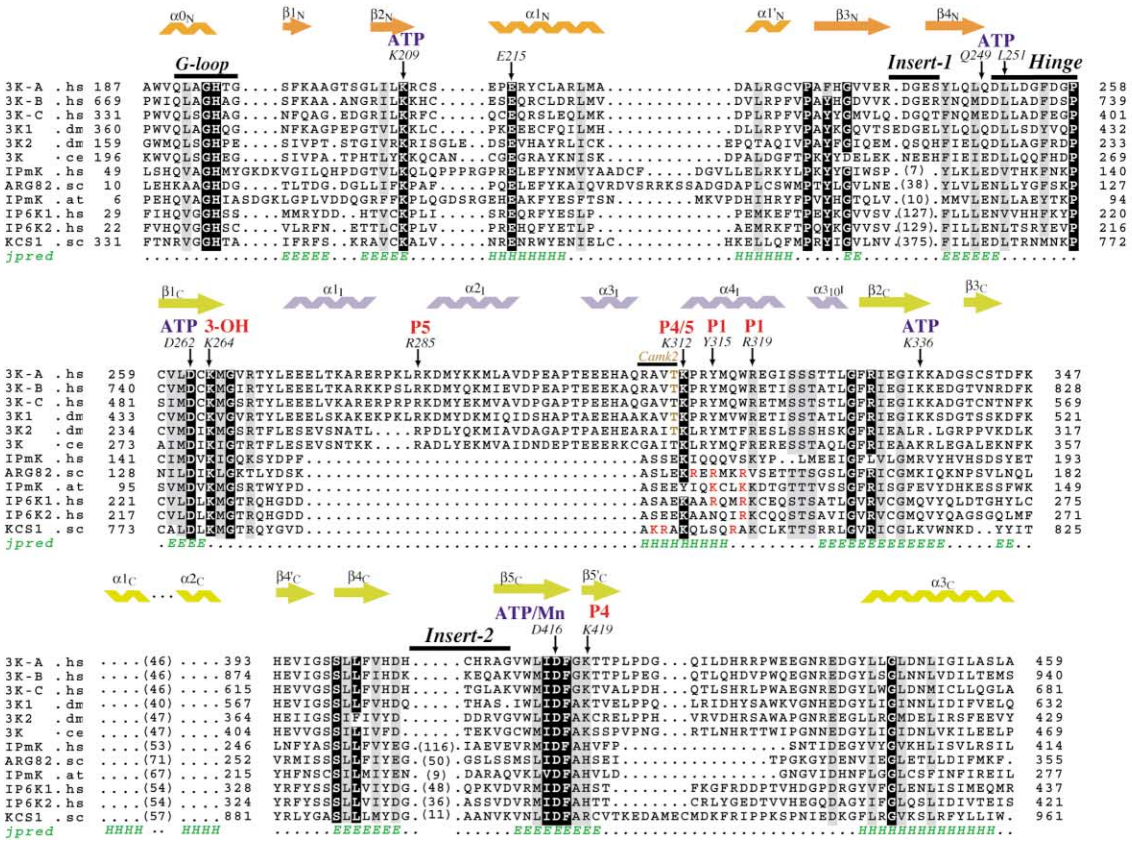


Figure 5. Structure-Based Comparison of the IPK Family

(A) A table showing the substrate specificities and reactions catalyzed by the IPK family members used for the alignment. A checkmark indicates a reaction catalyzed by an enzyme, and red checkmarks indicate the proposed main reactions occurring “in vivo” (Shears, 2004). The positions of the conserved motifs in each enzyme are also indicated.

shows additional structural similarity to IP₃-3K in the C-terminal lobe (Figure 1C). This enzyme also has a predominately β sheet C lobe, but the topology differs from IP₃-3K. Like IP₃-3K, PIPKII β has a shorter catalytic loop than the PKs (Figure 4C). PIPKII β also has a DxK₂₁₈ motif that is analogous to the DxK₂₆₄ motif of the IP₃-3Ks, and a Ser-Asp bridge between the SLL and DxK motifs is present in both enzymes. The similarity of key features suggests a close evolutionary relationship between the PIPKII β and IP₃-3K.

The fold of PIPKII β has been classified in a subfamily that is intermediate between the PK and ATP-grasp folds (Cheek et al., 2002; Grishin, 1999; Lo Conte et al., 2002). The only protein kinase member of this subfamily is the TRP channel kinase, ChaK (Yamaguchi et al., 2001). We propose that IP₃-3K is also a member of this subfamily. Consistent with this, the β strand connections of IP₃-3K C lobe are more similar to the ATP-grasp family (Grishin, 1999) than the connections present in PIPKII β , while the N lobe of IP₃-3K is more similar to PKs than the N lobe of PIPKII β . This makes IP₃-3K a closer link between the PK and ATP-grasp folds and supports the proposal that the ATP-grasp proteins and PKs diverged from a common ancestor (Grishin, 1999).

The IP binding lobe which is inserted in the IP₃-3K C lobe is an elaboration that is unique for IP₃-3K. The IP lobe is inserted in the middle of the β sheet between strands $\beta 1_C$ and $\beta 2_C$, while the substrate binding loop in PKs and lipid kinases is the loop that follows the last strand of the C lobe β sheet, also known as the “activation” loop (Pirola et al., 2001; Taylor and Radzio-Andzelm, 1994; Walker et al., 1999). As mentioned previously, one of the two residues interacting directly with the Ins(1,4,5) P_3 that comes from a subdomain other than the IP lobe is Lys419. This residue is in a C lobe region analogous to the activation loop of PKs, and points to only a limited similarity in substrate recognition compared with PKs and phosphoinositide kinases.

Catalytic Mechanism

The structures of the substrate and product complexes for IP₃-3K suggest some aspects of a catalytic mechanism. The 3-OH of Ins(1,4,5) P_3 substrate is 3.7 Å from the γ -phosphate of the ATP and the nearest oxygen of the 3-phosphate of the Ins(1,3,4,5) P_4 product is 3.9 Å from the β -phosphate of ADP. The proximity of the

γ -phosphate position in the ATP to its final position in the product is supportive of a direct “in-line” mechanism of phosphoryl transfer, as is the case for the PKA. Whether phosphoryl transfer proceeds along an associative or dissociative path awaits additional structural and biochemical data.

A key role in the IP₃-3K catalytic mechanism is played by Lys264. This residue, which interacts with 3-OH in the substrate complex and with the 3-phosphate in the product complex, is likely also to facilitate nucleophilic attack by neutralizing the negative charge developed in the transition state and by orienting the transferred phosphate. This role would be analogous to the role of Lys168 of PKA (Madhusudan et al., 2002). PKA has an additional key catalytic residue, Asp166 that forms a closer interaction with the serine hydroxyl. The main role of Asp166 is to select the correct rotamer of the substrate serine OH and thereby facilitate the nucleophilic attack by the hydroxyl (Madhusudan et al., 2002). In IP₃-3K, there is no residue equivalent to PKA Asp166; however, because of the differences in substrates, a need for such a residue is diminished, since the inositol ring greatly restricts the conformational freedom of the Ins(1,4,5) P_3 3-hydroxyl in comparison with the three highly populated χ_1 rotamers of a serine hydroxyl.

Apo Form versus Holo Form

The apo form versus substrate- or product-bound structures of IP₃-3K show intriguing conformational changes. Substrate-induced movement of the IP lobe helices reshape the substrate binding pocket: helix α_2 slides toward the bound InsP, while helices α_1 and α_4 tilt away from the inositide. A direct salt link between IP lobe residue Glu274 (helix α_1) and C lobe residue Lys419 is replaced by inositide-mediated interactions upon binding substrate. These conformational changes are necessary to lower the floor and shift a side wall of the binding pocket to provide sufficient space to accommodate the Ins(1,4,5) P_3 and to establish the specific interactions with its phosphates (Supplemental Figure S3). Both the product and substrate complexes show similar differences with respect to the apo-enzyme.

The most striking conformational change induced by substrates/products is that the N-terminal portion comprising residues 187 to 196 becomes disordered, whereas it is a defined α -helix (α_{0N}) in the apo form (Figure 3D).

(B) Schematic diagram of common IPK catalytic domain structural elements. The three major subdomains of the IPKs are color coded as in the other figures. Hatched lines indicate non-conserved insert regions, and the numbers over these regions indicate the range in the number of residues observed among all identifiable IPKs. Flagged regions indicate conserved motifs present in most IPK members.

(C) Sequence alignment of some representative IPKs. The first five sequences shown are IP₃-3Ks, the next three are IPmKs, and the bottom three are IP₆-Ks. Crucial amino acids involved in substrate binding are indicated above the alignment, with ATP binding residues in blue and Ins(1,4,5) P_3 binding residues in red. The observed secondary structure of human IP₃-3K-A is indicated above the alignments, while the green lettering below the alignments indicates secondary structure predictions done with the JPred server (<http://www.compbio.dundee.ac.uk>) on an alignment of the non-IP₃-3K sequences shown. Note that the C lobe helices α_{1C} and α_{2C} are shown only diagrammatically, since they cannot be aligned easily by primary sequence, despite having a common predicted secondary structure. CamK2 phosphorylation sites present in some, but not all IP₃-3Ks are indicated in brown just N-terminal to helix α_4 (the phosphorylated residue is T311 in human IP₃-3K A). Putative InsP binding residues present in the sole α -helix of the IP lobe of non-IP₃-3Ks are indicated in red. Alignments were performed using ClustalX, hand-adjusted with Indonesia, and colored in MacBoxshade. Accession numbers: human IP₃-3K A (3K-A.hs), NP_002211; human IP₃-3K B (3K-B.hs), CAC40650; human IP₃-3K C (3K-C.hs), NP_079470; *D. melanogaster* IP₃-3K, type 1 (3K1.dm), AAL89896; *D. melanogaster* IP₃-3K, type 2 (3K2.dm), AAL29155; *C. elegans* IP₃-3K form 1 (3K.ce), T42444; human IPmK (IPmK.hs), NP_689416; *S. cerevisiae* IPmK (ARG82.sc), NP_010458; *A. thaliana* IPmK 2A(IPmK.at), NP_196354; human IP₆-K 1 (IP6K1.hs), NP_695005; human IP₆-K 2 (IP6K2.hs), NP_057375; *S. cerevisiae* IP₆-K (KCS1.sc), NP_010300.

Surprisingly, this helix occupies the same site as the ATP molecule and residues from it interact with the rest of the enzyme in a manner that mimics the interactions that ATP makes. The indole moiety of Trp188 of α_{0N} occupies the same hydrophobic pocket as the adenine moiety of ATP, and it even makes a similar hydrogen bond with the enzyme (NE1 Trp188 - CO Gln 249, Figure 3D). This residue is conserved among the IP₃-3Ks. His194 is hydrogen bonded to the Asp416 in the ID₄₁₆FG motif through its NE2, and this residue is conserved among most members of the IPK family. These intramolecular interactions interfere with access to key residues for the enzyme catalysis and might be suggestive of a regulatory mechanism in the context of the full-length enzyme (see below).

Regulation by Ca²⁺/CAM Binding

IP₃-3Ks are regulated by Ca²⁺ in two ways. Mammalian isoforms A and B bind Ca²⁺/CAM, leading to an increase in V_{max}, and they are also phosphorylated and activated by Ca²⁺/CAM kinase II (CamK2) (Communi et al., 1995, 1997). Residues 158-174 have been implicated in Ca²⁺/CAM binding and IP₃-3K activation (Takazawa and Erneux, 1991). Reported activities of truncated variants of the enzyme are consistent with the region from 174-186 acting as an autoinhibitory segment (Takazawa and Erneux, 1991). The ordered N terminus that we see occupying the ATP binding pocket in the absence of substrate (187-196) suggests that this region might represent an additional portion of the autoinhibitory segment. Given that the construct we crystallized is nearly as active as constructs with an intact CAM binding domain after activation by Ca²⁺/CAM binding (Takazawa and Erneux, 1991), it appears that this additional segment is not sufficient on its own to inhibit the enzyme. Furthermore, a single point mutation within this segment, W188A did not lead to an increase in basal activity, but rather caused a slight decrease in activity, possibly by enzyme destabilization (Table 2). This proposed autoinhibitory mechanism is reminiscent of that observed for Twitchin (Kobe et al., 1996) and for CaMKI (Goldberg et al., 1996). These kinases also show an autoregulatory sequence binding in the active site to block ATP and substrate binding. We propose that a change in the accessibility of the ATP binding pocket caused by release of the autoinhibitory region could contribute to activation of IP₃-3K by Ca²⁺/CAM.

The location of the CamK2 phosphorylation site, Thr 311 in human isoform A (in the IP binding lobe, immediately N-terminal to helix α_4), is adjacent to an intramolecular salt link between Arg 314 and Glu 304 that probably rigidifies the IP binding lobe. The effect of phosphorylation may be to weaken this link allowing helix α_4 to more freely move relative to α_2 , a motion that we see accompanies Ins(1,4,5)P₃ binding. This model might explain the reported increase in sensitivity to CAM and increase in V_{max} reported to occur upon CamK2 phosphorylation (Communi et al., 1997).

IPK Family

Among the kinases that phosphorylate InsPs, IP₃-3K shows sequence similarity to both IPmKs and IP₆-Ks, and together they form the IPK family (Saiardi et al.,

1999; Schell et al., 1999; York et al., 1999). Because IP₃-3K is an enzyme found only in metazoans (the most primitive known example occurs in *C. elegans*), while both IP₆-K and IPmK occur also in plants and protists, it is assumed that IP₃-3K is a recent evolutionary elaboration on a more ancient IPK structure, which had either IPmK activity, IP₆-K activity, or both. In light of the inability of IP₃-3K to generate PtdIns(3,4,5)P₃, it appears that IP₃-3K evolved after PtdIns(3,4,5)P₃ had acquired a second messenger function (Irvine and Schell, 2001) so that this inability is an important part of the IP₃-3K biology.

A structure-based sequence alignment of IPKs reveals numerous common structural elements among IPKs, and also some intriguing differences (Figure 5). We propose that every major structural hallmark defined for IP₃-3K in the N lobe, IP lobe, and C lobe occurs in some form in all other IPKs. Indeed, secondary structure predictions are consistent with the idea that almost every α helix and β strand in IP₃-3K is recapitulated in the N and C lobes of all IPKs, including the three helices in the C lobe that confer structural support (α_{1C} , α_{2C} , and α_{3C}) (Figure 5B).

IP₃-3K is unique among protein and lipid kinases in that it has a separate substrate binding lobe, which is a flexible region of four helices rich in basic residues that contribute most of the specificity for Ins(1,4,5)P₃ recognition. This region is found in all IPKs, but in IPKs other than IP₃-3Ks the IP lobe is significantly smaller. Secondary structure prediction carried out on an alignment of 57 IPKs from various phyla supports the presence of one conserved α -helix, rich in basic residues in all IPK family members (not shown). This predicted primordial IP lobe is probably analogous to helix α_4 of IP₃-3K, which is responsible for most of the interactions with Ins(1,4,5)P₃. In this context, the exquisite specificity of IP₃-3K for Ins(1,4,5)P₃ compared to other IPKs (Figure 5A) would be due to the considerably greater structural constraints conferred by the additional helices in the IP lobe. Further specificity may be achieved by combination of negative selectivity due to C lobe residue Glu333, which is present only in IP₃-3Ks and would prevent IPmK and IP₆-K activity (Figure 5A) and positive selectivity due to the 4-phosphate ligand Lys419, which is a histidine in most other IPKs (Figure 5C).

The high selectivity of IP₃-3Ks contrasts with that of mammalian IPmKs, which in vitro exhibit kinase activity with at least seven different IP substrates and can catalyze at least eight distinct phosphorylation reactions (Chang et al., 2002; Saiardi et al., 1999, 2001; Shears, 2004). The smaller lobe of IPmK might form a less constrained pocket, allowing for multiple substrate orientations, as previously suggested (Shears, 2004). IPmKs can also function as a lipid kinase to catalyze the 3-phosphorylation of PtdIns(4,5)P₂ (A. Resnick, A. Saiardi, and S.H. Snyder, personal communication). This ability is most likely explained by the much smaller IP binding lobe lacking extensive 1-phosphate interactions.

IPKs kinase domain can also be distinguished by the differing locations of large inserts (Figures 5B and 5C). For example, in the kinase domain, IP₆-Ks have a variable insert, up to 376 residues, between strands β_3 and β_4 in the N lobe. In contrast, the equivalent N-terminal inserts of IPmKs are very short, 38 residues in ARG82 and up to 10 residues in other IPmKs. IPmKs and IP₆-

Ks, but not IP₃-3Ks, often have a second large insert located in a C lobe region distant from the catalytic site. Clues about the function of this insert come from the yeast ARG82, which in this region contains a patch of acidic residues that mediates interaction with transcription factors (Dubois et al., 2000; Irvine and Schell, 2001). A putative role of these insert regions in various aspects of nuclear functions is consistent with the previous suggestion that the first IPKs arose to subservise IP metabolism and signaling in the nucleus, while the evolution of IP₃-3Ks occurred later, around the same time as Ins(1,4,5) P_3 -mediated calcium signaling in the cytosol (Irvine and Schell, 2001).

Conclusions

The structure of the IP₃-3K shows how the enzyme achieves its remarkable substrate specificity that distinguishes it from the chemically related PI 3-kinase catalysis. In the context of this structure, it becomes possible to model a broad family of InsP kinases and to propose a model for the mechanism of activation by Ca²⁺/CAM. The phenotypes of cells with targeted deletions of IP₃-3K isoform B suggest that the enzyme has a pivotal role in T cell differentiation. A structural understanding of the specificity and mechanism of IP₃-3K may facilitate future studies aimed at establishing the molecular basis of its role in T cell development.

Experimental Procedures

Protein Purification

A construct consisting of residues 187–461 (187 to the C terminus) of human IP₃-3K-A with an N-terminal GST-tag and an A187S mutation was amplified from MGC clone 4792595 and cloned into the pOPTG vector. The protein was expressed in either *E. coli* C41(DE3) or the methionine auxotroph B834(DE3). Cells were grown at 37°C to OD₆₀₀ = 1.0 then induced with 0.3 mM IPTG for 15 hr at 16°C. Cells were resuspended in buffer A (20 mM Tris pH 7.5 [4°C], and 100 mM NaCl) and disrupted with a French press. The high-spin supernatant was loaded in batch onto Glutathione Sepharose4B. The resin was washed with buffer B (50 mM Tris [pH 7.5] and 200 mM NaCl). The protein was cleaved from the resin overnight at 4°C with TEV at a protease/sample mass ratio of 1/80. The cleaved protein was further purified on a 5 ml HiTrap heparin column followed by gel filtration on a 16/60 Superdex 75 column equilibrated in buffer D [20 mM Tris (pH 7.5) (4°C), 0.05 M (NH₄)₂SO₄, and 2 mM DTT]. IP₃-3K was concentrated to 28 mg/ml, frozen in liquid nitrogen, and stored at -70°C.

For enzyme assays, a construct consisting of residues 151 to the C terminus of human IP₃-3K with an N-terminal MetAla(His)₆-tag was used. Mutants were prepared by overlapping PCR. The proteins were purified by immobilized metal-affinity chromatography, desalted on PD10 columns equilibrated with buffer D, and frozen in liquid nitrogen.

Analytical Ultracentrifugation

Sedimentation equilibrium experiments were done in Beckman Optima XL-I ultracentrifuge with a Ti-60 rotor using interference and absorbance at 280 and 230 nm, at 10°C. The protein was loaded into 6-sector 12 mm path length cells at 3 μM, 15 μM, and 300 μM. The samples were spun at 30,000, 37,000, and 45,000 rpm until they reached equilibrium.

Crystallization

Initially, 1440 conditions were screened in 96-well crystallization plates (Corning), using 100 nl drops dispensed by a Cartesian robot (Genomics Solutions, UK). Optimal crystals were obtained at 17°C in 1 μl sitting drops over reservoirs of 24-well plates (Hampton) containing a reservoir solution consisting of 0.83–0.85 M tri-sodium

citrate, 0.1 M Tris-HCl (pH 8.0) (r.t.) and 0.1 M NaCl. To prepare complexes of the crystals with heavy atom derivatives, substrates and products, a 1 μl aliquot of a soaking solution consisting of 2 M Li₂SO₄ and 100 mM Tris-HCl (pH 8) (4°C) was added to the drop and 1 μl was then removed. This addition/removal was repeated 7 times and then crystals were soaked in the final solution for 2.5 hr. Crystals were frozen by dunking them in liquid nitrogen. To prepare crystals of a substrate complex, the soaking solution also contained 3 mM AMPPNP, 3 mM MnCl₂, and 10 mM Ins(1,4,5) P_3 (Alexis). To prepare crystals of product complex, the soaking solution contained 3 mM ADP (Sigma), 3 mM MnCl₂, and 5 mM Ins(1,3,4,5) P_4 (Alexis). Products were also formed in situ when the soaking solution contained 3 mM ATP, 3 mM MnCl₂, and 5 mM Ins(1,4,5) P_3 .

Data Collection, Phasing, and Model Refinement

Data were collected at 100 K. The enzyme crystallized in space group C222, with cell parameters $a = 72.3$, $b = 98.2$, $c = 190.7$. A trimethyl lead acetate (TMLA) derivative was obtained by incubating crystals for 3.5 hr in soaking solution with 5 mM TMLA and 20 mM LuCl₃. Data sets were collected at wavelengths corresponding to the fluorescence peak and the inflection. A total of 13 sites were located and refined by a combination of SOLVE (Terwilliger and Berendzen, 1999) and autoSHARP (de La Fortelle and Bricogne, 1997). Solvent flattening was carried out using a solvent content of 49.6% as optimized by SHARP. The electron density map was easily interpretable (Supplemental Figure S4). Table 1 lists statistics for data collection and phase refinement.

High-resolution data sets were collected for the apo-enzyme crystal from selenomethionine-substituted protein, a Mn²⁺/AMPPNP/Ins(1,4,5) P_3 complex (substrate complex) and a Mn²⁺/ADP/Ins(1,3,4,5) P_4 complex (product complex). Preliminary models for these data sets were obtained using Arp/warp with an initial electron density map calculated from heavy-atom-derived phases combined with observed amplitudes. These models were then optimized with cycles of manual fitting and refinement with REFMAC. Final statistics for all data sets are given in Table 1. There are no residues in the disallowed regions of the Ramachandran plot and 89% of residues are in the most favored regions as defined by PROCHECK. Residues 187–196 of the substrate and product-bound complexes are not ordered for either of the two molecules in the asymmetric unit. For molecule B, residues 278–282 and 298–308 are not ordered in the substrate and product complexes.

Acknowledgments

We thank Olga Perisic for help with many aspects of the work and Alexey Murzin for useful discussions. We thank Joanne McCarthy, Ed Mitchell, and Andrew McCarthy for assistance with data collection at ESRF beamlines ID14-2, ID14-4, and ID29, respectively. B.G.P. was supported by a fellowship from Secretaría de Estado de Educación y Universidades and co-financed by the European Social Fund. The work was supported by the Wellcome Trust (R.F.I. and A.J.L.), the Royal Society (M.J.S. and R.F.I.), and the MRC (R.L.W.).

Received: May 20, 2004

Revised: June 29, 2004

Accepted: July 1, 2004

Published: online: August 12, 2004

References

- Balla, T., Sim, S.S., Baukal, A.J., Rhee, S.G., and Catt, K.J. (1994). Inositol polyphosphates are not increased by overexpression of Ins(1,4,5) P_3 3-kinase but show cell-cycle dependent changes in growth factor-stimulated fibroblasts. *Mol. Biol. Cell* 5, 17–27.
- Berridge, M.J. (1993). Inositol trisphosphate and calcium signalling. *Nature* 361, 315–325.
- Bertsch, U., Deschermeier, C., Fanick, W., Girkontaite, I., Hillemeier, K., Johnen, H., Weglohner, W., Emmrich, F., and Mayr, G.W. (2000). The second messenger binding site of inositol 1,4,5-trisphosphate 3-kinase is centered in the catalytic domain and related to the inositol trisphosphate receptor site. *J. Biol. Chem.* 275, 1557–1564.

- Bird, G.S., Obie, J.F., and Putney, J.W., Jr. (1992). Sustained Ca²⁺ signaling in mouse lacrimal acinar cells due to photolysis of "caged" glycerophosphoryl-myo-inositol 4,5-bisphosphate. *J. Biol. Chem.* 267, 17722–17725.
- Bosanac, I., Alattia, J.R., Mal, T.K., Chan, J., Talarico, S., Tong, F.K., Tong, K.L., Yoshikawa, F., Furuichi, T., Iwai, M., et al. (2002). Structure of the inositol 1,4,5-trisphosphate receptor binding core in complex with its ligand. *Nature* 420, 696–700.
- Chang, S.C., Miller, A.L., Feng, Y., Wente, S.R., and Majerus, P.W. (2002). The human homolog of the rat inositol phosphate multikinase is an inositol 1,3,4,6-tetrakisphosphate 5-kinase. *J. Biol. Chem.* 277, 43836–43843.
- Cheek, S., Zhang, H., and Grishin, N.V. (2002). Sequence and structure classification of kinases. *J. Mol. Biol.* 320, 855–881.
- Choi, K.Y., Kim, H.K., Lee, S.Y., Moon, K.H., Sim, S.S., Kim, J.W., Chung, H.K., and Rhee, S.G. (1990). Molecular cloning and expression of a complementary DNA for inositol 1,4,5-trisphosphate 3-kinase. *Science* 248, 64–66.
- Clandinin, T.R., DeModena, J.A., and Sternberg, P.W. (1998). Inositol trisphosphate mediates a RAS-independent response to LET-23 receptor tyrosine kinase activation in *C. elegans*. *Cell* 92, 523–533.
- Communi, D., Takazawa, K., and Erneux, C. (1993). Lys-197 and Asp-414 are critical residues for binding of ATP/Mg²⁺ by rat brain inositol 1,4,5-trisphosphate 3-kinase. *Biochem. J.* 291, 811–816.
- Communi, D., Vanweyenberg, V., and Erneux, C. (1995). Molecular study and regulation of D-myo-inositol 1,4,5-trisphosphate 3-kinase. *Cell. Signal.* 7, 643–650.
- Communi, D., Vanweyenberg, V., and Erneux, C. (1997). D-myo-inositol 1,4,5-trisphosphate 3-kinase A is activated by receptor activation through a calcium:calmodulin-dependent protein kinase II phosphorylation mechanism. *EMBO J.* 16, 1943–1952.
- Cullen, P.J., Hsuan, J.J., Truong, O., Letcher, A.J., Jackson, T.R., Dawson, A.P., and Irvine, R.F. (1995). Identification of a specific Ins(1,3,4,5)P₄-binding protein as a member of the GAP1 family. *Nature* 376, 527–530.
- de La Fortelle, E., and Bricogne, G. (1997). Maximum-likelihood heavy-atom parameter refinement for multiple isomorphous replacement and multiwavelength anomalous diffraction methods. *Methods Enzymol.* 276, 472–494.
- Dewaste, V., Pouillon, V., Moreau, C., Shears, S., Takazawa, K., and Erneux, C. (2000). Cloning and expression of a cDNA encoding human inositol 1,4,5-trisphosphate 3-kinase C. *Biochem. J.* 352, 343–351.
- Dewaste, V., Moreau, C., De Smedt, F., Bex, F., De Smedt, H., Wuytack, F., Missiaen, L., and Erneux, C. (2003). The three isoenzymes of human inositol-1,4,5-trisphosphate 3-kinase show specific intracellular localization but comparable Ca²⁺ responses on transfection in COS-7 cells. *Biochem. J.* 374, 41–49.
- Dubois, E., Dewaste, V., Erneux, C., and Messenguy, F. (2000). Inositol polyphosphate kinase activity of Arg82/ArgR113 is not required for the regulation of the arginine metabolism in yeast. *FEBS Lett.* 486, 300–304.
- Dubois, E., Scherens, B., Vierendeels, F., Ho, M.M., Messenguy, F., and Shears, S.B. (2002). In *Saccharomyces cerevisiae*, the inositol polyphosphate kinase activity of Kcs1p is required for resistance to salt stress, cell wall integrity, and vacuolar morphogenesis. *J. Biol. Chem.* 277, 23755–23763.
- Goldberg, J., Nairn, A.C., and Kuriyan, J. (1996). Structural basis for the autoinhibition of calcium/calmodulin-dependent protein kinase I. *Cell* 84, 875–887.
- Grishin, N.V. (1999). Phosphatidylinositol phosphate kinase: a link between protein kinase and glutathione synthase folds. *J. Mol. Biol.* 291, 239–247.
- Ho, M.W., Yang, X., Carew, M.A., Zhang, T., Hua, L., Kwon, Y.U., Chung, S.K., Adelt, S., Vogel, G., Riley, A.M., et al. (2002). Regulation of Ins(3,4,5,6)P(4) signaling by a reversible kinase/phosphatase. *Curr. Biol.* 12, 477–482.
- Huse, M., and Kuriyan, J. (2002). The conformational plasticity of protein kinases. *Cell* 109, 275–282.
- Irvine, R.F., and Schell, M.J. (2001). Back in the water: the return of the inositol phosphates. *Nat. Rev. Mol. Cell Biol.* 2, 327–338.
- Irvine, R.F., Letcher, A.J., Heslop, J.P., and Berridge, M.J. (1986). The inositol tris/tetrakisphosphate pathway—demonstration of Ins(1,4,5)P₃ 3-kinase activity in animal tissues. *Nature* 320, 631–634.
- Ives, E.B., Nichols, J., Wente, S.R., and York, J.D. (2000). Biochemical and functional characterization of inositol 1,3,4,5, 6-pentakisphosphate 2-kinases. *J. Biol. Chem.* 275, 36575–36583.
- Jun, K., Choi, G., Yang, S.G., Choi, K.Y., Kim, H., Chan, G.C., Storm, D.R., Albert, C., Mayr, G.W., Lee, C.J., et al. (1998). Enhanced hippocampal CA1 LTP but normal spatial learning in inositol 1,4,5-trisphosphate 3-kinase(A)-deficient mice. *Learn. Mem.* 5, 317–330.
- Kobe, B., Heierhorst, J., Feil, S.C., Parker, M.W., Benian, G.M., Weiss, K.R., and Kemp, B.E. (1996). Giant protein kinases: domain interactions and structural basis of autoregulation. *EMBO J.* 15, 6810–6821.
- Lemmon, M.A., and Ferguson, K.M. (2001). Molecular determinants in pleckstrin homology domains that allow specific recognition of phosphoinositides. *Biochem. Soc. Trans.* 29, 377–384.
- Lo Conte, L., Brenner, S.E., Hubbard, T.J., Chothia, C., and Murzin, A.G. (2002). SCOP database in 2002: refinements accommodate structural genomics. *Nucleic Acids Res.* 30, 264–267.
- Madhusudan, Trafny, E.A., Xuong, N.H., Adams, J.A., Teneyck, L.F., Taylor, S.S., and Sowadski, J.M. (1994). cAMP-dependent protein kinase-crystallographic insights into substrate recognition and phosphotransfer. *Protein Sci* 3, 176–187.
- Madhusudan, Akamine, P., Xuong, N.H., and Taylor, S.S. (2002). Crystal structure of a transition state mimic of the catalytic subunit of cAMP-dependent protein kinase. *Nat. Struct. Biol.* 9, 273–277.
- Mailleux, P., Takazawa, K., Erneux, C., and Vanderhaeghen, J.J. (1991). Inositol 1,4,5-trisphosphate 3-kinase distribution in the rat brain. High levels in the hippocampal CA1 pyramidal and cerebellar Purkinje cells suggest its involvement in some memory processes. *Brain Res.* 539, 203–210.
- Morris, A.J., Murray, K.J., England, P.J., Downes, C.P., and Michell, R.H. (1988). Partial purification and some properties of rat brain inositol 1,4,5-trisphosphate 3-kinase. *Biochem. J.* 251, 157–163.
- Nalaskowski, M.M., Bertsch, U., Fanick, W., Stockebrand, M.C., Schmale, H., and Mayr, G.W. (2003). Rat inositol 1,4,5-trisphosphate 3-kinase C is enzymatically specialized for basal cellular inositol trisphosphate phosphorylation and shuttles actively between nucleus and cytoplasm. *J. Biol. Chem.* 278, 19765–19776.
- Odom, A.R., Stahlberg, A., Wente, S.R., and York, J.D. (2000). A role for nuclear inositol 1,4,5-trisphosphate kinase in transcriptional control. *Science* 287, 2026–2029.
- Pattni, K., and Banting, G. (2004). Ins(1,4,5)P(3) metabolism and the family of IP(3)-3Kinases. *Cell. Signal.* 16, 643–654.
- Pirola, L., Zvelebil, M.J., Bulgarelli-Leva, G., Van Obberghen, E., Waterfield, M.D., and Wymann, M.P. (2001). Activation loop sequences confer substrate specificity to phosphoinositide 3-kinase α (PI3K α). *J. Biol. Chem.* 276, 21544–21554.
- Pouillon, V., Hascakova-Bartova, R., Pajak, B., Adam, E., Bex, F., Dewaste, V., Van Lint, C., Leo, O., Erneux, C., and Schurmans, S. (2003). Inositol 1,3,4,5-tetrakisphosphate is essential for T lymphocyte development. *Nat. Immunol.* 4, 1136–1143.
- Rao, V.D., Misra, S., Boronenkov, I.V., Anderson, R.A., and Hurley, J.H. (1998). Structure of type II β phosphatidylinositol phosphate kinase: a protein kinase fold flattened for interfacial phosphorylation. *Cell* 94, 829–839.
- Saiardi, A., Erdjument-Bromage, H., Snowman, A.M., Tempst, P., and Snyder, S.H. (1999). Synthesis of diphosphoinositol pentakisphosphate by a newly identified family of higher inositol polyphosphate kinases. *Curr. Biol.* 9, 1323–1326.
- Saiardi, A., Nagata, E., Luo, H.R., Sawa, A., Luo, X., Snowman, A.M., and Snyder, S.H. (2001). Mammalian inositol polyphosphate multikinase synthesizes inositol 1,4,5-trisphosphate and an inositol pyrophosphate. *Proc. Natl. Acad. Sci. USA* 98, 2306–2311.
- Schell, M.J., Letcher, A.J., Brearley, C.A., Biber, J., Murer, H., and

Irvine, R.F. (1999). PiUS (Pi uptake stimulator) is an inositol hexakisphosphate kinase. *FEBS Lett.* **461**, 169–172.

Schell, M.J., Erneux, C., and Irvine, R.F. (2001). Inositol 1,4,5-trisphosphate 3-kinase A associates with F-actin and dendritic spines via its N terminus. *J. Biol. Chem.* **276**, 37537–37546.

Shears, S.B. (2004). How versatile are inositol phosphate kinases? *Biochem. J.* **377**, 265–280.

Takazawa, K., and Erneux, C. (1991). Identification of residues essential for catalysis and binding of calmodulin in rat brain inositol 1,4,5-trisphosphate 3-kinase. *Biochem. J.* **280**, 125–129.

Taylor, S.S., and Radzio-Andzelm, E. (1994). Three protein kinase structures define a common motif. *Structure* **2**, 345–355.

Terwilliger, T.C., and Berendzen, J. (1999). Automated structure solution for MIR and MAD. *Acta Crystallogr. D* **55**, 849–861.

Togashi, S., Takazawa, K., Endo, T., Erneux, C., and Onaya, T. (1997). Structural identification of the myo-inositol 1,4,5-trisphosphate-binding domain in rat brain inositol 1,4,5-trisphosphate 3-kinase. *Biochem. J.* **326**, 221–225.

Verbsky, J.W., Wilson, M.P., Kisseleva, M.V., Majerus, P.W., and Wenthe, S.R. (2002). The synthesis of inositol hexakisphosphate. Characterization of human inositol 1,3,4,5,6-pentakisphosphate 2-kinase. *J. Biol. Chem.* **277**, 31857–31862.

Walker, E.H., Perisic, O., Ried, C., Stephens, L., and Williams, R.L. (1999). Structural insights into phosphoinositide 3-kinase catalysis and signalling. *Nature* **402**, 313–320.

Wen, B.G., Pletcher, M.T., Warashina, M., Choe, S.H., Ziaee, N., Wiltshire, T., Sauer, K., and Cooke, M.P. (2004). Inositol (1,4,5) trisphosphate 3 kinase B controls positive selection of T cells and modulates Erk activity. *Proc. Natl. Acad. Sci. USA* **101**, 5604–5609.

Wilson, M.P., and Majerus, P.W. (1996). Isolation of inositol 1,3,4-trisphosphate 5/6-kinase, cDNA cloning and expression of the recombinant enzyme. *J. Biol. Chem.* **271**, 11904–11910.

Yamada, M., Kakita, A., Mizuguchi, M., Rhee, S.G., Kim, S.U., and Ikuta, F. (1992). Ultrastructural localization of inositol 1,4,5-trisphosphate 3-kinase in rat cerebellar cortex. *Brain Res.* **578**, 41–48.

Yamaguchi, H., Matsushita, M., Nairn, A.C., and Kuriyan, J. (2001). Crystal structure of the atypical protein kinase domain of a TRP channel with phosphotransferase activity. *Mol. Cell* **7**, 1047–1057.

York, J.D., Odom, A.R., Murphy, R., Ives, E.B., and Wenthe, S.R. (1999). A phospholipase C-dependent inositol polyphosphate kinase pathway required for efficient messenger RNA export. *Science* **285**, 96–100.

Yoshimura, K., Watanabe, Y., Erneux, C., and Hirata, M. (1999). Use of phosphorofluoridate analogues of D-myo-inositol 1,4,5-trisphosphate to assess the involvement of ionic interactions in its recognition by the receptor and metabolising enzymes. *Cell. Signal.* **11**, 117–125.

Accession Numbers

The coordinates of the structures described here have been deposited in the Protein Data Bank. The entry codes are 1w2f (apoenzyme), 1w2c (Mn²⁺/AMPPNP/Ins(1,4,5)P₃ complex), and 1w2d (Mn²⁺/ADP/Ins(1,3,4,5)P₄ complex).